



# On-chip acoustic mixer integration of electro-microfluidics towards in-situ and efficient mixing in droplets

Yao Lu<sup>1</sup> · Menglun Zhang<sup>1</sup> · Hongxiang Zhang<sup>1</sup> · Jingze Huang<sup>1</sup> · Zhan Wang<sup>1</sup> · Zelin Yun<sup>1</sup> · Yanyan Wang<sup>1</sup> · Wei Pang<sup>1</sup> · Xuexin Duan<sup>1</sup> · Hao Zhang<sup>1</sup>

Received: 3 May 2018 / Accepted: 22 November 2018 / Published online: 28 November 2018  
© Springer-Verlag GmbH Germany, part of Springer Nature 2018

## Abstract

Rapid and reliable micromixing requires continuous improvement to renovate more powerful microfluidics chip for chemosynthesis, biological assay, and drug purification. In this work, we realized rapid in-situ mixing in droplets on a closed electro-microfluidic chip. Electrowetting and 2.5 GHz acoustic wave streaming were coupled into a monolithic chip for the manipulation and active mixing of microdroplets, respectively. Finite-element analysis simulation provided three-dimensional illustrations of turbulent flow pattern, fluid velocity, and vortices core locations. We carried out mixing experiments on different scales from nanoscale molecules to microscale particles, accelerating mixing efficiency by more than 50 times compared with pure diffusion. In the enzyme catalytic reaction experiment for biological assay demonstration, mixing efficiency of biological samples improves by about one order of magnitude compared with conventional 96-well-plate assay. Limited temperature rising of mixing in microdroplets validates biological safety, which guarantees potentials of the chip in various biochemical analyses and medical applications.

**Keywords** Electrowetting-on-dielectric · In-situ mixing · Active mixer · Acoustofluidics · Integrated biochip

## 1 Introduction

Microfluidic technology, operating and analyzing fluids on microscale, has made significant development from the early 1980s in lab-on-a-chip (LOC) and micrototal analysis system ( $\mu$ TAS) (Darwin Reyes et al. 2002; Whitesides 2011). To fulfill such complicated applications, basic microfluidic

operations are essential on a chip and include dispersing, mixing, separating, injecting, and delivering. Of these operations, mixing of analytes or reagents is a crucial step in chemical reaction (Hiromitsu et al. 2015; Kim et al. 2016), biological assay (Lynn et al. 2014), particles manipulation (Liu et al. 2015), nanomaterial synthesis (Valencia et al. 2018; Wang et al. 2014), and protein study (Li et al. 2014). Microfluidic mixing in volume of  $\mu$ L to pL leads to low-efficiency mixing due to low Reynolds number regimes in micron and nanoscale devices (Beebe et al. 2002).

**Electronic supplementary material** The online version of this article (<https://doi.org/10.1007/s10404-018-2169-7>) contains supplementary material, which is available to authorized users.

✉ Menglun Zhang  
zml@tju.edu.cn

✉ Wei Pang  
weipang@tju.edu.cn

Yao Lu  
luyao@tju.edu.cn

Hongxiang Zhang  
tjzhx@tju.edu.cn

Jingze Huang  
huangjingze@tju.edu.cn

Zhan Wang  
zhanwang@tju.edu.cn

Zelin Yun  
cloud9477@163.com

Yanyan Wang  
yanyanwang@tju.edu.cn

Xuexin Duan  
xduan@tju.edu.cn

Hao Zhang  
haozhang@tju.edu.cn

<sup>1</sup> State Key Laboratory of Precision Measuring Technology and Instruments, Tianjin University, Tianjin 300072, China

In recent years, various microfluidic mixing strategies have been developed to realize homogeneous mixing in shorter time for miniaturized and easy-to-use microfluidic chip (Hessel et al. 2005; Suh and Kang 2010). Current mixing schemes are generally categorized as active mixing (Hessel et al. 2005; Oberti et al. 2009; Suh and Kang 2010; Neild et al. 2010) and passive mixing (Hessel et al. 2005; Suh and Kang 2010; Lee et al. 2016) according to the introduction of external energy. The strategies in passive mixing mainly focus on embedded barriers (Le The et al. 2015) and geometric topology (Lee et al. 2009; Hong et al. 2016) of microchannels to produce chaotic mixing or laminar mixing, and its mixing efficiency relies on pumping pressure, flow-rate control, and geometric design. Besides, the three-dimensional structure of microchannels cannot be reconstructed and the fabrication is non-trivial (Lim et al. 2011). On the other hand, active mixing typically has higher mixing efficiency due to the introduction of external energy or actuators, such as pressure (Glasgow and Aubry 2003), thermal (Tsai and Lin 2002), electrodynamics (El Moctar et al. 2003), electrokinetics (Chang and Yang 2007), electrowetting (Mugele et al. 2011), dielectrophoresis (Viehwies et al. 2012), magnetodynamics (Chen et al. 2013), and ultrasonic (Yang et al. 2001). For the electrical mixing methods, the mixed media are limited to conducting liquid (Chun et al. 2008). For magnetic-force method including magnetic-bead mixing, assistant complex manipulation is needed (Ballard et al. 2016). Generally speaking, acoustic mixing is advantageous in application scope. Physical properties of mixed media are not limited due to a universal mechanical force applied by acoustic waves. In addition, the non-contact mixing by acoustic wave is safe in biological (e.g., cell) and chemical applications (Xie et al. 2012; Wiklund 2012). In the acoustic mixing category, surface acoustic wave (SAW) has long been studied (Frommelt et al. 2008; Ding et al. 2013; Yeo and Friend 2014; Fu et al. 2017). Piezoelectric transducer (PZT) has also been incorporated into microfluidics to generate acoustic streaming and mixing (Madison et al. 2017). Compared with the above two strategies, thin-film-type device fabricated by MEMS technology as another avenue has the advantages of smaller size ( $\sim \mu\text{m}$ ) and higher frequency ( $\sim \text{GHz}$ ) (Pang et al. 2012; Zhang et al. 2017), which might contribute to high level of integration for on-chip applications and large acoustic streaming force for higher vortices velocity ( $\sim \text{m/s}$ ). However, in the realm of acoustic mixing, the research on GHz acoustic mixing (Cui et al. 2016; Qu et al. 2017; Wang et al. 2017) is still limited.

Most active and passive mixing are carried out in microchannel chips, which need external pumping and controlling components, like pumps and valves. Besides, mixing also requires a lengthy microchannel to flow through which takes up a large portion of the chip. Thus, droplet-operation form is necessary for portable multi-sample handling. As an

alternative approach, electrofluidics based on electrowetting-on-dielectric (EWOD) is a microdroplets manipulation technology free from pumps and valves. Electrofluidic chip can control microdroplets individually, and reconfigure position and actions of microdroplets on-demand (Cho et al. 2003). These features make electrofluidics ideal for LOC applications (Jebrail et al. 2012; Samiei et al. 2016). However, electrofluidics, lacking of pumping pressure, cannot adopt passive mixing strategy. In addition, electrofluidics calls for in-situ mixing to get rid of lengthy microchannels.

In this paper, EWOD droplet manipulation and active acoustic micromixers were integrated in a monolithic electrofluidic chip as a new strategy for on-chip mixing. Ultrahigh frequency ( $\sim 2.5 \text{ GHz}$ ) piezoelectric resonators as acoustic micromixers were excited to produce turbulent flow in microdroplets for in-situ, pumping-free, and highly efficient mixing. In addition, multiple droplets can be manipulated by EWOD actuator in multiplexed approach to satisfy other basic microfluidic operations. The in-situ mixing strategy and compact integration greatly improves the area utilization and functions of chip. The integrated electrofluidic chip can target a wide range of synthesis and analysis applications for LOC and  $\mu\text{TAS}$ .

## 2 Chip design and experimental methods

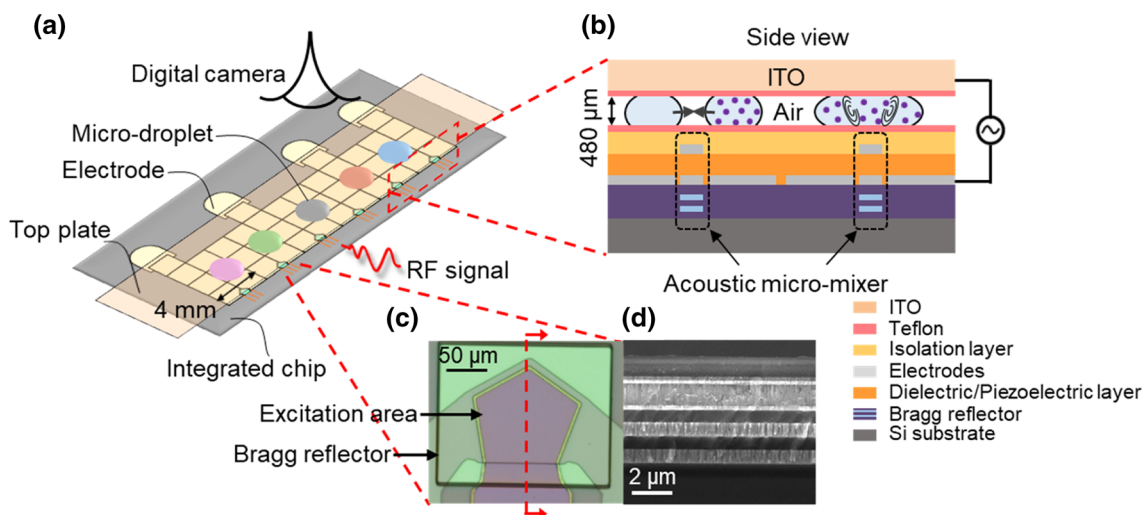
### 2.1 Mixing principle

The on-chip mixing strategy consists of droplets merging via EWOD effect and acoustic streaming mixing. EWOD, as a kind of electrofluidic technologies, operates droplets to generate, transport, merge and mix, through modulating the solid–liquid surface tension with alternative current (AC) power, which is applied on the electrodes of EWOD (Cho et al. 2003). Based on the fluids manipulation capabilities of EWOD, acoustic micromixers are further combined for rapid in-situ mixing of merged microdroplets. The micromixer is designed based on the converse piezoelectric effect of piezoelectric materials, generating ultrasonic waves with radio-frequency (RF) signal applied on it. The intense mechanical vibration of micromixer reaches the peak under its nature frequency, where the acoustics wave will be excited. When the micromixer is immersed in liquid circumstance, most acoustic energy leaks into liquid due to low reflection coefficient at liquid–solid interface, resulting violent microvortex in liquid, which was defined as acoustic streaming effect (Friend and Yeo 2011). Based on this concept, the integrated electrofluidic chip, adopting EWOD and acoustic streaming technologies, could operate multiple microdroplets flexibly and satisfy the need of mixing for different samples simultaneously.

The schematic of a closed electrofluidic chip is shown in Fig. 1a, showing two parallel plates with sandwiched multiple microdroplets. Bottom plate (2.4 cm W × 3.7 cm L) integrates EWOD (forty-four 2 mm × 2 mm electrodes) and six acoustic micromixers, which process virtues of compact integration and parallel multi-droplet operation. Four larger electrodes of EWOD are designed as reservoirs for continuous samples loading and collecting. The power supplied on the responding electrode pads (not shown) of EWOD for manipulate droplets is AC. The whole top plate is indium–tin–oxide (ITO) glass as the ground electrode of EWOD, forming a closed chip with bottom plate together. The cross-sectional view of the closed integrated chip is presented in Fig. 1b. The structure of EWOD includes positive electrodes, dielectric layer, and hydrophobic film. The acoustic micromixer consists of a sandwiched structure (bottom electrode, piezoelectric layer, and top electrode) and Bragg reflector to reflect acoustic waves (Enlund et al. 2008; Chen et al. 2010). The sharing of the same thin film (orange part in Fig. 1b) between piezoelectric layer of micromixer and dielectric layer of EWOD is the key to compact integration. The enlarged view (Fig. 1c) of micromixer was captured by microscope. The longitudinal wave is excited in the designed pentagon area, aimed to avoid spurious mode caused by acoustic interference and determining the position of acoustic vortices in microdroplet. Moreover, the cross-sectional view (Fig. 1d) of micromixer presents the detailed information of each layer, corresponding to each layer in Fig. 1b. Based on the construction of integrated chip, the process of in-situ mixing is shown in Fig. 2, in

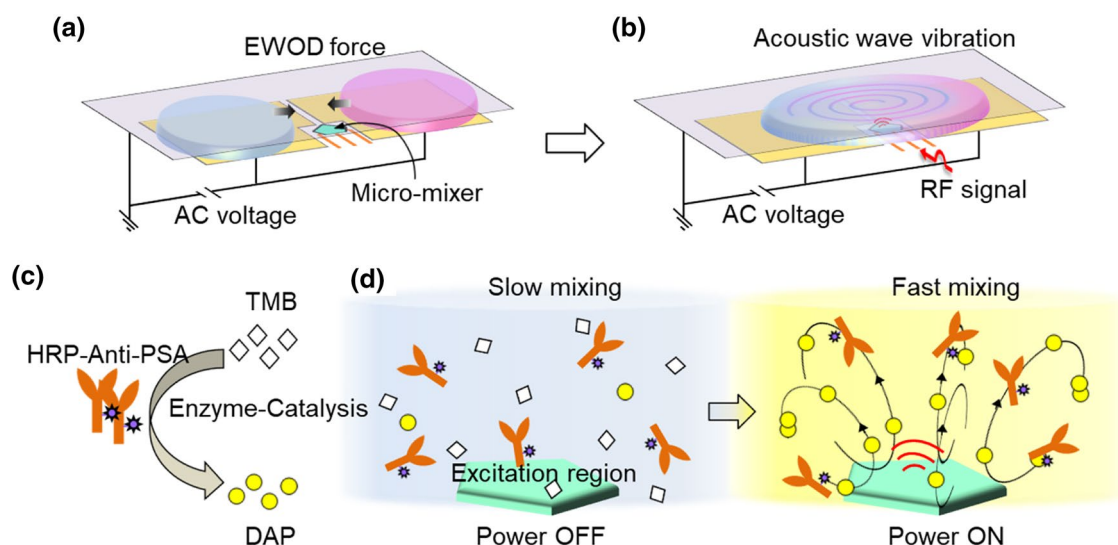
which two different microdroplets are driven to merge along the patterned electrodes via EWOD force (Fig. 2a). Then, AC power is turned off and RF signal is transmitted into micromixer to implement the in-situ mixing via acoustic streaming, as shown in Fig. 2b. When the mixing is completed, the new microdroplet could be driven to other areas of the electrofluidic chip for further operations. In addition to acoustic mixing, EWOD-force mixing and pure diffusion have been studied and compared with acoustic mixing to analyze their mixing efficiency. For EWOD-force mixing, the merged droplet is driven (1 Hz) forward and backward on three electrodes by EWOD force to accelerate the mixing. For pure diffusion, the merged droplet does not move, and the mixing is accomplished by pure diffusion force without external perturbation.

The integrated electrofluidic chip, capable of on-chip droplet operation (parallel transporting, rapid mixing), should cater the applications in the biological field. For some biochemical reactions, reducing mixing time is preferable for assays to avoid excessive internal or external disturbance, since some products will degrade or oxidize very quickly with reaction proceeding. In this work, the mixing of bio-molecules based on enzymic catalytic reaction commonly used in enzyme-linked immunosorbent assay (ELISA) was studied. The reaction needs enzyme and substrate reagents as reactants and the substrate will change into a colored product by enzyme catalysis. The amount of the product directly relates to the amount of the target substances in the sample, and could be qualitatively or quantitatively analyzed according to the depth of the color reaction. Qualitative test



**Fig. 1** **a** Illustration of the integrated electrofluidic chip, consisting closed EWOD structure (bottom chip and top plate) and six embedded micromixers: several microdroplets are loaded on the closed chip; the mixing processes are recorded by a digital camera. The size of EWOD electrodes is 2 mm × 2 mm. **b** Side view of integrated chip: the merging and mixing of two different microdroplets by EWOD

effect and acoustic streaming, respectively. The gap between bottom chip and top plate is 480 μm. **c** Top view of the micromixer under optical microscope: the pentagon area is the acoustic excitation region and the rectangular area is Bragg reflector. **d** Sectional view of the micromixer by scanning electron microscope (SEM), corresponding to each layer in **b**



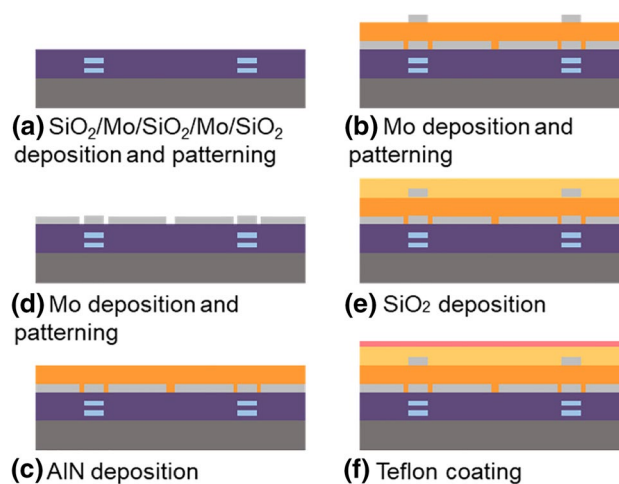
**Fig. 2** **a** Process of in-situ mixing on closed electrofluidic chip with a micromixer embedded between adjacent electrodes of EWOD. Merging the two microdroplets via EWOD effect with AC power applied on the electrodes, and then **b** mixing the merged droplet via acoustic streaming induced by micromixer with RF power input. **c** Schematic

diagram of mixing of bio-molecules in enzymic catalytic reaction. The substrate (TMB) changes from colorless to yellow (DAP) under the catalysis of enzyme (HRP). **d** Comparison between pure diffusion under RF power OFF and acoustic streaming under RF power-ON

was used in this paper to determine whether the target substances (antigen or antibody) are present in the specimen. Figure 2c shows the schematic diagram of enzymic catalytic reaction using tetramethylbenzidine (TMB) and horseradish peroxidase (HRP) as substrate and catalytic agent, respectively. Prostate-specific antigen (PSA), labeled with HRP as the target substance, was evaluated by the colored product (2,3-diamino-phenazin, DAP) as illustrated above. When this reaction proceeds in a static liquid circumstance, the thoroughgoing color turning is slow due to free diffusion, as described in Fig. 2d (left). However, the interaction process will be accelerated when bio-molecules are forced to collide with the appearance of extra flow induced by acoustic wave, as described in right of Fig. 2d.

## 2.2 Device fabrication

The fabrication of the integrated chip, as summarized in Fig. 3, was based on the standard MEMS microfabrication technology. The  $\text{SiO}_2/\text{Mo}/\text{SiO}_2/\text{Mo}/\text{SiO}_2$  acoustical Bragg reflector was deposited on the Si substrate ( $400\ \mu\text{m}$ ) for effective acoustic energy reflection (Fig. 2a). The thickness of each layer was  $1/4\ \lambda$ . Molybdenum (Mo) layer ( $200\ \mu\text{m}$ ) was sputtered and patterned (Fig. 3b), forming the actuation electrodes ( $2\ \text{mm} \times 2\ \text{mm}$ ) of EWOD and the bottom electrodes of the acoustic micromixers. Then, highly *c*-axis-oriented polycrystalline aluminum nitride (AlN) film ( $1.1\ \mu\text{m}$ ) was deposited (Fig. 3c). Afterwards, another Mo layer ( $200\ \mu\text{m}$ ) was deposited and patterned to form the top electrodes of the acoustic micromixers (Fig. 3d). Thus, a



**Fig. 3** Illustration of the fabrication process

sandwich structure (Mo–AlN–Mo) of the micromixer was formed. To improve device reliability, silicon dioxide ( $1\ \mu\text{m}$ ) as isolation layer was further deposited above the AlN film (Fig. 3e). TiW ( $100\ \text{nm}$ ) and Au ( $300\ \text{nm}$ ) were successively deposited on the electrodes of micromixers for RF signal transmission (not shown). Finally, 1% Teflon ( $\sim 30\ \text{nm}$ ) as the hydrophobic film of EWOD was spin-coated (Fig. 3f) and baked for 15 min at  $165\ ^\circ\text{C}$ . In all experiments, ITO glass ( $8.5\ \text{cm W} \times 1\ \text{cm L}$ ) was used as the ground electrode of EWOD and also processed with Teflon. Double-sided tapes as spacer were placed between ITO glass and bottom plate.



### 2.3 Measurement setup

The mixing efficiency of molecules and particles in microdroplets was measured by comparing pure diffusion, conventional mixing, and acoustic streaming methods. The integrated chip was assembled on an evaluation board, and the micromixers bonded with Au wires were connected to RF signal generator (N5172B EXG, Agilent) and power amplifier (Mini-Circuits, ZHL-5W-422). For peripheral control, we used PC and relay switch circuit to control the power supply of each EWOD electrode. The power supply of AC signal generator (GFG-8015G, GW Instek) was 70–90 V<sub>rms</sub>, 1 KHz. The size of the gap (480 μm) between top plate and bottom chip together with the EWOD electrodes (2 mm) defines the volume of microdroplet (~2.5 μL). After the setup and samples were prepared, we set the control procedure of EWOD on the PC and then loaded samples on the reservoirs. After that, the automatic operation could be conducted as the above-mentioned principle of in-situ mixing. The whole on-chip operation process was recorded by a fixed digital camera (EOS-550D, Nikon) above the integrated chip with resolution of 25 frames per second. In addition, a thermal imaging camera (CEM DT-980) was also fixed above the chip to measure the temperature of microdroplets under different RF powers.

### 2.4 Model simulation

To investigate flow-field distribution induced by acoustic micromixer, we carried out a three-dimensional simulation by finite-element analysis using turbulent flow module. A finite water domain with 4 mm length, 2 mm width, and 480 μm height above the pentagon region was established, consistent with the size of microdroplet in the experiments. The body force equation (Cui et al. 2016) was introduced at pentagon region to characterize the acoustic streaming effect in the liquid area, and all boundaries were set as slip condition. The piezoelectric acoustic device can excite ~2.5 GHz longitudinal waves that mainly propagate along z-axis direction and dissipate in the liquid. The dissipation of the acoustic wave was converted to the kinetic energy of fluid, and turbulent module was used to analyze the vortex velocity distributions induced by acoustic streaming.

### 2.5 Normalized mixing characterization

We used MATLAB software to process selected pictures acquired from digital camera. The characterization of mixing was based on the uniformity of color in the whole merged droplet. We extracted the color changes in RGB, and computed its mean values of all pixels for the selected frames. As the mixing goes on, the mean color values tend to be constant (i.e., the color no longer changes), defined as final

state. Thus, the deviations of mean color values between each frames and final state represent the unmixed portion. By calculating the ratio of deviations to the final state, we can get normalized indices to characterize mixing state at different times. The expression of normalized mixing index (NMI) is as follows:

$$\text{NMI} = 1 - \frac{\frac{1}{N} \sum_{i=1}^N I'_i - \frac{1}{N} \sum_{i=1}^N I_i}{\frac{1}{N} \sum_{i=1}^N I_i}, \quad (1)$$

where  $I'_i$  and  $I_i$  are the RGB color intensity value of the  $i$ th pixel of unmixed states and final states, respectively, while  $N$  is the number of pixels of selected region.

### 2.6 Solutions

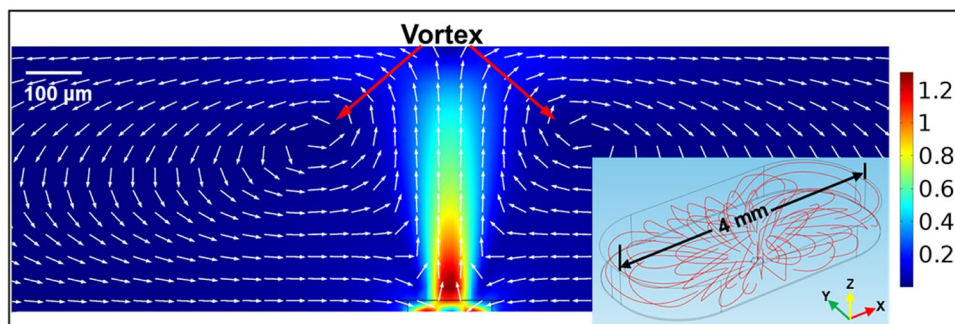
Tetramethylbenzidine (TMB) and horseradish peroxidase (HRP) were purchased from Shanghai Linc-Bio Science Co., Ltd. The TMB solution used in our experiments was diluted to ten times. Polystyrene (PS) particles (5 μm dia.) were purchased from BioScientific, Gynea NSM. Phenolphthalein was purchased from Shanghai Yuanye Bio-Technology Co., Ltd. Alkaline solution (pH 10) was compounded by sodium bicarbonate (NaHCO<sub>3</sub>) buffer and sodium carbonate (NaCO<sub>3</sub>) buffer. Pluronic F-68 powder was purchased from Shanghai yuanye Bio-Technology Co., Ltd. We dissolved pluronic F-68 in deionized (DI) water to prepare 0.2% (w/v) pluronic F-68 solution.

## 3 Results and discussion

### 3.1 Finite-element analysis simulation

Figure 4 shows the flow pattern and velocity distribution in the plane perpendicular to the surface of pentagon at 300 mW power input. It is clear that the acoustic flows rise up from the bottom of liquid and rotate clockwise or counterclockwise to the surroundings of the device, forming two symmetrical vortices in the interior of liquid. A three-dimensional simulation (the inset) of the turbulent flows vividly describes different sizes of streaming lines at any plane in the whole flow field. As we can see, the maximum of the simulated streaming velocity (1.31 m/s) occurs at the edge of the device. Reynolds number calculated by the maximum velocity is 3275, larger than the critical value (2300) in laminar flow (Beebe et al. 2002), which further proves that the fluid flows in this system are turbulent flows. These simulated results prove the feasibility of using acoustic actuator for liquid mixing.

**Fig. 4** Simulation results of the turbulent mode when micro-mixer is immersed in water: flows pattern and velocity field of acoustic streaming. Inset is the three-dimensional acoustic streaming distribution of 480  $\mu\text{m}$  above the acoustic device



### 3.2 Nanoscale molecular mixing

Colorimetric pH experiments were conducted to validate the molecular mixing ability of this integrated electrofluidic chip. Two 2.3  $\mu\text{L}$  microdroplets (indicator and test agent) were loaded on the chip separately, and driven to ( $U_{\text{rms}} = 70 \text{ V}$ , 1 KHz) merge via EWOD force. The gap height was set to 480  $\mu\text{m}$ . Figure 5 describes the colorimetric pH measurements with phenolphthalein solution (with additive 0.2% w/v pluronic F-68) and alkaline solution (pH 10, with additive 0.2% w/v pluronic F-68). The reaction began at the moment of merging, and shows amaranth color at the region, where two solutions completely mixed. We defined the moments when two droplets collide together as  $t=0 \text{ s}$  for each mixing experiment.

Figure 5a shows a series of pictures showing the progress of pure diffusion in static-merged droplet. The reaction was still incomplete after 6.5 min. Figure 5b details a conventional mixing method usually used in EWOD mixing: the EWOD force moved the merged droplet forward and backward (1 Hz) to speed up mixing. Although the molecular interactions were accelerated by the electro-hydrodynamic force of EWOD, it still needed 33 s to finish 99% mixing, as the normalized index of mixing process shown. Figure 5c illustrates the acoustic mixing and normalized mixing index with time: EWOD force actuated two microdroplets merging, and then, micromixer began to work under 300 mW RF power input. The violent acoustic streaming produced by the propagation of acoustic wave in liquid accelerated the molecular interactions, taking 8 s to complete 99% mixing. The results indicate that the mixing efficiency via acoustic streaming is more than 50 times higher than pure diffusion method and three times higher than the conventional EWOD-mixing method.

### 3.3 Microscale particle mixing

For the mixing in micron scales, 5  $\mu\text{m}$  dia. polystyrene (PS) particles were used to feature the mixing process in a merged droplet. The mixing of micron particles is more challenging in practical applications because of low diffusion coefficient,

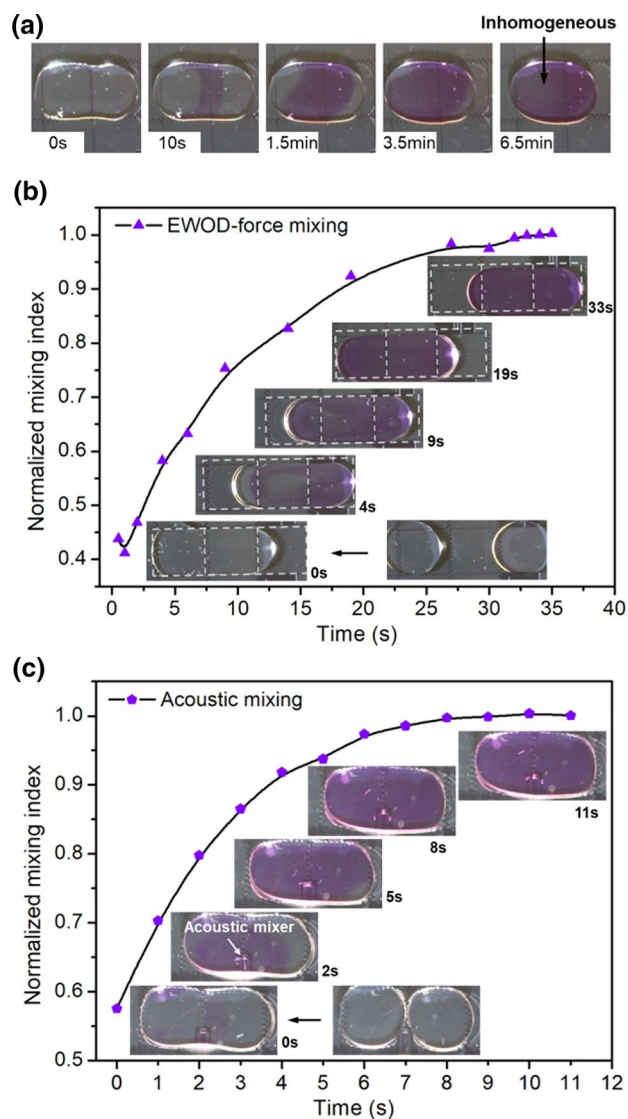


**Fig. 5** Characterization of molecular-scale mixing for colorimetric pH measurement after the coalition of phenolphthalein solution (left: 2.3  $\mu\text{L}$ ) and alkaline solution (right: pH 10, 2.3  $\mu\text{L}$ ), using **a** pure diffusion, **b** conventional EWOD mixing by driving the merged droplet forward and backward, and **c** acoustic mixing via the propagation of acoustic wave

non-negligible gravity, and complicated collision. As shown in Fig. 6a, EWOD force ( $U_{rms} = 80$  V, 1 KHz) pulled the two aqueous microdroplets together of which one contained PS particles, and then driven the merged droplet moving forward and backward. Quite a few of PS particles were pushed into left from right (driving towards the right) at  $t = 7$  s, while most of them returned back to their original position basically (driving towards the left) at  $t = 8$  s because of the round trip of flow. Thus, the conventional EWOD-mixing method requires particles to take more time to reach a uniform distribution. The total time was about 35 s for complete EWOD mixing using the closed electrofluidic chip. Besides, it is difficult for particles to launch pure diffusion due to the excessive mass of particle after driving to merge by EWOD force.

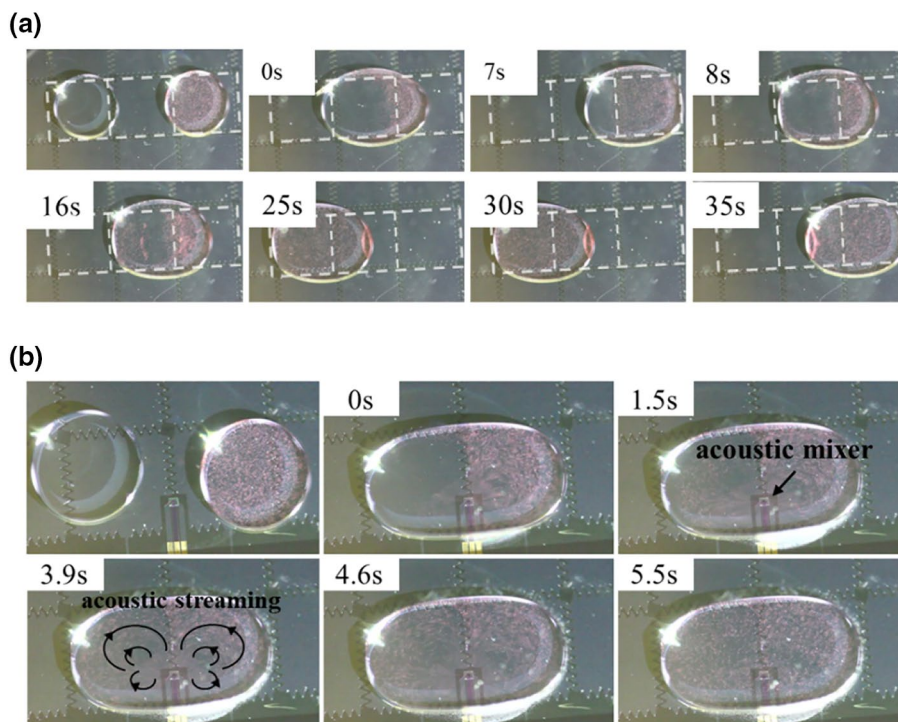
In the acoustic mixing method, particles in acoustic wave field are subject to four forces: gravity force, buoyant force, acoustic radiation force, and streaming-induced drag force. The gravity force and buoyant force are almost balanced, because the density of PS particle ( $1.05 \text{ g/cm}^3$ ) is very close to water. Based on the Stoke’s law for plane sine wave propagation in isotropic and homogeneous medium (Stokes 1845), the acoustic waves decay exponentially along the direction perpendicular to device surface and can be approximated to zero in the region above  $50 \mu\text{m}$ . In the in-situ mixing system, the effect of acoustic radiation force can be neglected due to the larger liquid region ( $4 \text{ mm L} \times 2 \text{ mm W} \times 480 \mu\text{m H}$ ). Therefore, the movement of particles is mainly dominated by drag force. Figure 6b presents the result of particles in-situ

mixing via acoustic streaming. Similar to the previous steps, EWOD force driven the two microdroplets to merge, and then, acoustic wave created directional streaming which forced particles to the surroundings following the results of simulation. All the PS particles stopped moving after turning off the RF power (see the Electronic Supplementary Material). The acoustic mixing method of PS particles reduces the mixing time to 5 s, which improves the mixing efficiency by  $\sim 6$  times compared with the conventional EWOD-mixing method. Figure 7 shows the normalized evaluation curves of EWOD force and acoustic mixing efficiency, respectively. The oscillation of curve (EWOD-force mixing) comes from the repeated movement of particles driven by EWOD force (as in the case of  $t = 7$  s and  $t = 8$  s in Fig. 6a) and the awkward situation for extracting RGB colors from particles solution.

### 3.4 Enzyme catalytic mixing

The above-mixing results provided a further idea to demonstrate a practical biological assay for lab-on-a-chip applications. We performed the enzymic catalytic reaction on the integrated chip, as mentioned in Fig. 2c, d. Conventional well-plate assay for ELISA, relying on pure diffusion of bio-molecules, usually needs more than 10 min to reach a complete mixing. The similar pure diffusion process is shown in Fig. 8a. Microdroplets of samples containing TMB (left) and HRP-Anti-PSA (right) were driven to merge, and then, the catalytic reaction began based on the bio-molecule

**Fig. 6** Experimental validation of particle scale mixing in aqueous microdroplet. The sequence frames of **a** conventional EWOD mixing by driving the DI water (left:  $2.5 \mu\text{L}$ ) and PS particles ( $5 \mu\text{m}$ ) aqueous microdroplet (right:  $2.5 \mu\text{L}$ ) forward and backward and **b** in-situ acoustic mixing under 500 mW power input





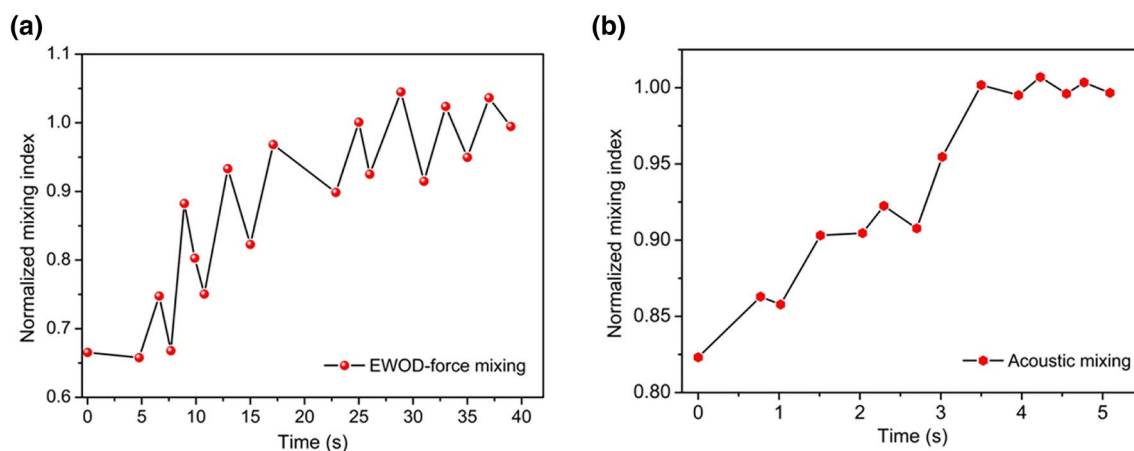


**Fig. 7** Mixing efficiency characterization of EWOD-force mixing **a** and acoustic mixing **b** for microscale particles

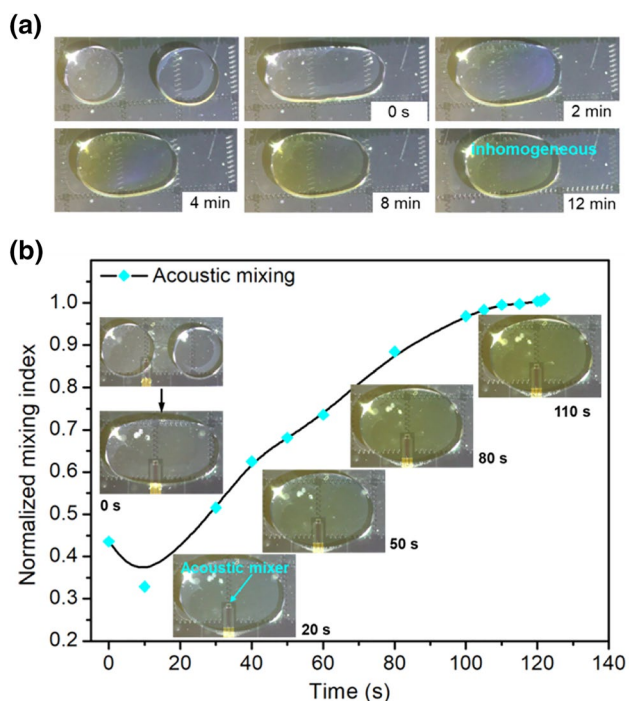


**Fig. 8** Application of rapid mixing for enzymic catalytic reaction on the electrofluidic chip. The sequence frames of **a** conventional well-plate assay based on pure diffusion after the coalition of TMB solution (left: 2.5  $\mu$ L) and HRP-Anti-PSA (right: 2.5  $\mu$ L) solution and **b** acoustic mixing due to the propagation of acoustic wave

interaction by pure diffusion. The reaction was still incomplete after 12 min. For EWOD-force mixing, the results are not presented here, because it is difficult to effectively drive the reagents droplets owing to the low contact angle of TMB reagent. However, for some bio-reagents droplets with relatively low surface tension, such as buffer, saline solution, and even cell-culture medium, the integrated chip is able to drive and merge the droplets, and hence, EWOD mixing is

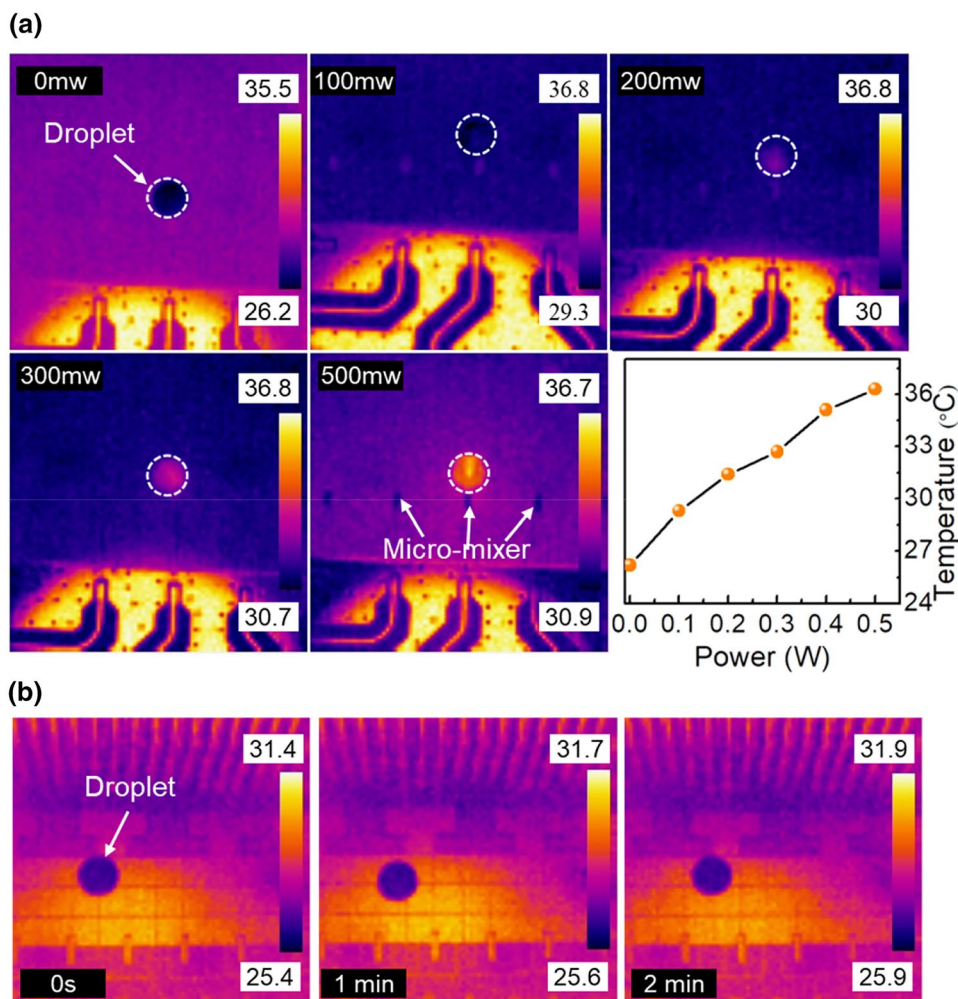
also feasible. In contrast, mixing of bio-molecules by acoustic streaming was carried out. Figure 8b shows the reaction process and normalized color characterization according to the above-normalized characterization: 99% catalytic reaction was completed at 110 s under 300 mW power input, which indicates an accelerated reaction efficiency by more than six times. Compared with the above-mixing experiments (particles and molecules), catalytic reaction is not a process of solely mixing, after which it takes a certain amount of time to react. The preliminary analysis demonstrates that bimolecular mixing via acoustic streaming on the integrated chip can be further used in biological assays.

## 4 Discussion

The above results demonstrate efficient in-situ mixing in different scales for on-chip sample preparation and analysis. Still, there are several aspects need to be taken into account for robustness and application scope. The acoustic energy transferred to the droplet will eventually produce heat in samples. With the increase of input power, the resulting heat will inevitably be a concern. The temperatures of the samples during mixing should be kept in a moderate range, because biological contents, such as proteins and enzyme, might lose activity due to excessive temperature. We measured the temperature of PBS sample using a thermal imaging camera with different powers applied to micromixer. Figure 9a shows the temperature measurements at 0 mW, 100 mW, 200 mW, 300 mW, and 500 mW after the temperature becomes stabilized. The highest temperature of sample goes to 36.3  $^{\circ}$ C at the power input of 500 mW. The maximum temperature increment of  $\sim 10$   $^{\circ}$ C is applicable for many biochemical reactions. For example, the activity of enzyme could reach highest at 37  $^{\circ}$ C. In addition, the temperature increment can be controlled by adjusting the



**Fig. 9 a** Temperature measurements of PBS microdroplet under different powers applied to micromixer. The measurements were performed after the temperature becomes stabilized. The data points in the temperature–power graph were obtained from the highest temperature of the microdroplet. **b** Temperature measurement of droplet by EWOD-force mixing during 2 min



input power. The adjustment of temperature could also be utilized in applications that need certain temperature to activate or accelerate specific reactions. Besides, for pure diffusion, the temperature of droplet is steady (i.e., 25.6 °C); For EWOD mixing, EWOD drives the droplets by changing the surface energy of liquid–solid interface, in which very little energy turns into heat. Thus, the temperature of droplet hardly changes (from 25.4 to 25.9 °C) after 2 min, as shown in Fig. 9b.

Since the acoustic streaming has a certain range of action, for the mixing in the microfluidic system, the boundary size of the microfluidics affects the position and velocity of vortices, which in turn affects the mixing effect. Different from PZT acoustic mixing (Madison et al. 2017), thin-film acoustic micromixer with higher frequency would produce larger body force to form violent acoustic streaming. On the other hand, the micromixing at open boundary (Qu et al. 2017; Wang et al. 2017) and in microchannel (Cui et al. 2016) has been reported. Differently, we investigated the flow velocity of in-situ microdroplet-mixing of different scales under closed boundary. A finite water domain with different

heights ( $z$ ) and fixed lateral sizes ( $x=4$  mm,  $y=2$  mm) was established. Figure 10a describes the changes of average velocity with the liquid height, with the flow velocity reaches maximum at  $\sim 0.5$  mm. Apart from the height factor, lateral dimension would also act on the flow velocity. Different lateral sizes of finite water domain were analyzed with fixed gap height ( $z=0.5$  mm), as the orange curve shows: the effects of lateral size ( $x$  or  $y$ ) within a reasonable range on flow velocity are almost negligible compared to the longitudinal. In addition, the vortices are farther and higher along  $x$  and  $z$  directions, as the gap height increases, as shown in Fig. 10b. From the perspective of external system, the gap height between the top plate and bottom chip is a dependent parameter for the mixing efficiency in microdroplet. In a word, the design of longitudinal and lateral dimension in closed boundary determines the flows and the patterns of vortices, which will further affect the mixing efficiency.

In another aspect, the acoustic streaming effect varies in different liquid properties, such as viscosity (molecular weight) and density. Therefore, in this work, the improvement of mixing efficiency at different scales is uneven. As

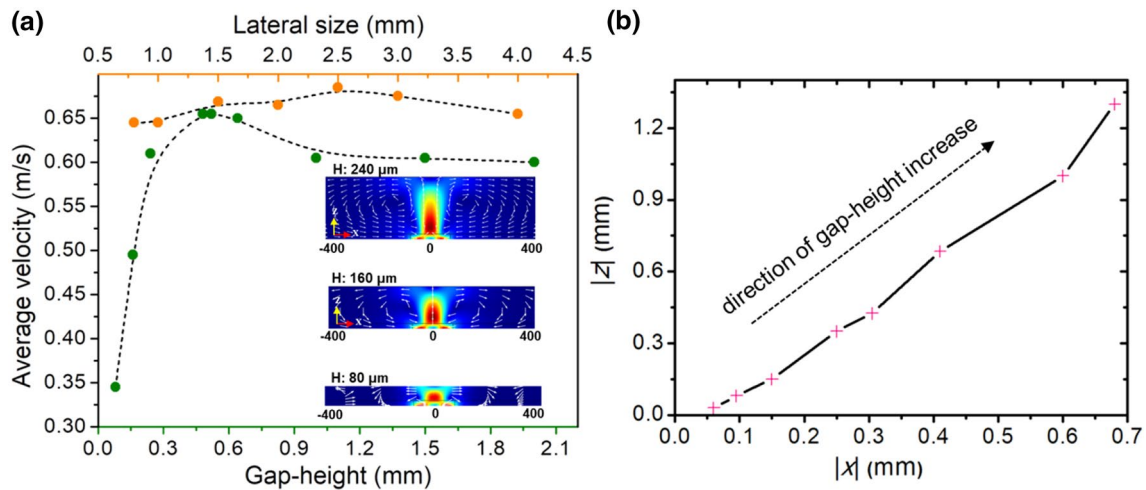


**Fig. 10** Simulation results of flow velocity with different dimensions of finite water domain. **a** Relationship between average velocity and different dimensions (height and lateral). **b** Position of vortex along  $x$  and  $z$  directions as the increase of gap height

the results of mixing experiments show, the mixing efficiency of acoustic mixing was increased by 50 times at small molecule scale, but six times at macromolecular scale, compared with pure diffusion. The mechanism will be further investigated and modeled in our future work. Meanwhile, the volume of sample will also change as height changes according to the driving principle in EWOD. Besides, the ratio of supplied power to the streaming velocity of fluids should be optimized for higher mixing efficiency and smaller temperature increment. Thus, the optimization of relevant parameters to further reduce the mixing time, droplet volume, and power consumption will be studied in our future work.

## 5 Conclusion

In summary, we reported a new strategy for on-chip, rapid, and in-situ mixing in microdroplets via integrating bulk acoustic wave micromixer array on a closed electrofluidic chip. Efficient mixing has been demonstrated in molecular scale and micron particles' solution, which greatly improves the mixing efficiency compared with pure diffusion and conventional EWOD-mixing methods. We demonstrated biological assay by accelerating the enzyme catalytic reaction. Besides, measurements of temperature in microdroplet validated that the heat produced by acoustic wave is controllable and moderate. These mixing results verify the availability and superiority of integrating  $\sim$  GHz acoustic micromixer with EWOD-based electrofluidics for efficient in-situ mixing. Further development and optimization of the chip will focus on faster mixing, smaller usage of reagents, lower consumption of power, and functional diversification

(e.g., sensing and heating), better qualified for practical LOC applications.

**Acknowledgements** The authors acknowledge financial support from the Natural Science Foundation of China (NSFC no. 51375341), the 111 Project (B07014), Nanchang Institute for Microtechnology of Tianjin University, and the National High Technology Research and Development Program of China (863 Program no. 2015AA042603).

## Compliance with ethical standards

**Conflict of interest** The authors declare that they have no conflict of interest.

**Research involving human participants and/or animals** None.

**Informed consent** Yes.

## References

- Ballard M, Owen D, Mills ZG et al (2016) Orbiting magnetic microbeads enable rapid microfluidic mixing. *Microfluid Nanofluid* 20:1–13. <https://doi.org/10.1007/s10404-016-1750-1>
- Beebe DJ, Mensing GA, Walker GM (2002) Physics and Applications of microfluidics in biology. *Annu Rev Biomed Eng* 4:261–286. <https://doi.org/10.1146/annurev.bioeng.4.112601.125916>
- Chang CC, Yang RJ (2007) Electrokinetic mixing in microfluidic systems. *Microfluid Nanofluid* 3:501–525. <https://doi.org/10.1007/s10404-007-0178-z>
- Chen D, Xu Y, Wang J et al (2010) The AlN based solidly mounted resonators consisted of the all-metal conductive acoustic Bragg reflectors. *VAC* 85:302–306. <https://doi.org/10.1016/j.vacuum.2010.07.001>
- Chen C-Y, Chen C-Y, Lin C-Y, Hu Y-T (2013) Magnetically actuated artificial cilia for optimum mixing performance in microfluidics. *Lab Chip* 13:2834. <https://doi.org/10.1039/c3lc50407g>
- Cho SK, Moon H, Chang-Jin Kim (2003) Creating, transporting, cutting, and merging liquid droplets by electrowetting-based

- actuation for digital microfluidic circuits. *J Microelectromech Syst* 12:70–80. <https://doi.org/10.1109/JMEMS.2002.807467>
- Chun H, Kim HC, Chung TD (2008) Ultrafast active mixer using polyelectrolytic ion extractor. *Lab Chip* 8:764. <https://doi.org/10.1039/b715229a>
- Cui W, Zhang H, Zhang H et al (2016) Localized ultrahigh frequency acoustic fields induced micro-vortices for submillisecond microfluidic mixing. *Appl Phys Lett*. <https://doi.org/10.1063/1.4972484>
- Darwin R, Reyes D, Iossifidis, Pierre-Alain Auroux † and, Manz\* A (2002) Micro total analysis systems. 1. Introduction, theory, and technology. <https://doi.org/10.1021/AC0202435>
- Ding X, Li P, Lin S-CS et al (2013) Surface acoustic wave microfluidics. *Lab Chip* 13:3626. <https://doi.org/10.1039/c3lc50361e>
- El Moctar AO, Aubry N, Batton J (2003) Electro-hydrodynamic microfluidic mixer electronic supplementary information (ESI) available: video of effect of electric field on channel flow mixing. See <http://www.rsc.org/suppdata/lc/b3/b306868b/>. *Lab Chip* 3:273. <https://doi.org/10.1039/b306868b>
- Enlund J, Martin D, Yantchev V, Katardjiev I (2008) Solidly mounted thin film electro-acoustic resonator utilizing a conductive Bragg reflector. *Sens Actuators A* 141:598–602. <https://doi.org/10.1016/j.sna.2007.09.002>
- Friend J, Yeo LY (2011) Microscale acoustofluidics: Microfluidics driven via acoustics and ultrasonics. *Rev Mod Phys* 83:647–704. <https://doi.org/10.1103/RevModPhys.83.647>
- Frommelt T, Kostur M, Wenzel-Schäfer M et al (2008) Microfluidic mixing via acoustically driven chaotic advection. *Phys Rev Lett* 100:1–4. <https://doi.org/10.1103/PhysRevLett.100.034502>
- Fu YQ, Luo JK, Nguyen NT et al (2017) Advances in piezoelectric thin films for acoustic biosensors, acoustofluidics and lab-on-chip applications. *Prog Mater Sci* 89:31–91. <https://doi.org/10.1016/j.pmatsci.2017.04.006>
- Glasgow I, Aubry N (2003) Enhancement of microfluidic mixing using time pulsing. *Lab Chip* 3:114–120. <https://doi.org/10.1039/B302569A>
- Hessel V, Löwe H, Schönfeld F (2005) Micromixers—a review on passive and active mixing principles. *Chem Eng Sci* 60:2479–2501. <https://doi.org/10.1016/j.ces.2004.11.033>
- Hiromitsu S, Jin K, Emiko S et al (2015) Novel method for immunofluorescence staining of mammalian eggs using non-contact alternating-current electric-field mixing of microdroplets. *Sci Rep* 5:1–10. <https://doi.org/10.1038/srep15371>
- Hong SO, Cooper-White JJ, Kim JM (2016) Inertio-elastic mixing in a straight microchannel with side wells. *Appl Phys Lett*. <https://doi.org/10.1063/1.4939552>
- Jebrail MJ, Bartsch MS, Patel KD (2012) Digital microfluidics: a versatile tool for applications in chemistry, biology and medicine. *Lab Chip* 12:2452. <https://doi.org/10.1039/c2lc40318h>
- Kim H, Min K-I, Inoue K et al (2016) Submillisecond organic synthesis: Outpacing Fries rearrangement through microfluidic rapid mixing. *Science* 352:691–694. <https://doi.org/10.1126/science.aaf1389>
- Le The H, Le Thanh H, Dong T et al (2015) An effective passive micromixer with shifted trapezoidal blades using wide Reynolds number range. *Chem Eng Res Des* 93:1–11. <https://doi.org/10.1016/j.CHERD.2014.12.003>
- Lee MG, Choi S, Park JK (2009) Rapid laminating mixer using a contraction–expansion array microchannel. *Appl Phys Lett* 95:1–4. <https://doi.org/10.1063/1.3194137>
- Lee CY, Wang WT, Liu CC, Fu LM (2016) Passive mixers in microfluidic systems: a review. *Chem Eng J* 288:146–160. <https://doi.org/10.1016/j.cej.2015.10.122>
- Li Y, Liu C, Feng X et al (2014) Ultrafast microfluidic mixer for tracking the early folding kinetics of human telomere G-quadruplex. *Anal Chem* 86:4333–4339. <https://doi.org/10.1021/ac500112d>
- Lim TW, Son Y, Jeong YJ et al (2011) Three-dimensionally crossing manifold micro-mixer for fast mixing in a short channel length. *Lab Chip* 11:100–103. <https://doi.org/10.1039/C005325M>
- Liu C, Hu G, Jiang X, Sun J (2015) Inertial focusing of spherical particles in rectangular microchannels over a wide range of Reynolds numbers. *Lab Chip* 15:1168–1177. <https://doi.org/10.1039/C4LC01216J>
- Lynn NS, Martínez-López JI, Bocková M et al (2014) Biosensing enhancement using passive mixing structures for microarray-based sensors. *Biosens Bioelectron* 54:506–514. <https://doi.org/10.1016/j.bios.2013.11.027>
- Madison AC, Royal MW, Fair RB et al (2017) Piezo-driven acoustic streaming in an electrowetting-on-dielectric digital microfluidics device. *Microfluid Nanofluid* 21:1–9. <https://doi.org/10.1007/s10404-017-2012-6>
- Mugele F, Staicu A, Bakker R, van den Ende D (2011) Capillary Stokes drift: a new driving mechanism for mixing in AC-electrowetting. *Lab Chip*. <https://doi.org/10.1039/c0lc00702a>
- Neild A, Ng TW, Sheard GJ et al (2010) Swirl mixing at microfluidic junctions due to low frequency side channel fluidic perturbations. *Sens Actuators B* 150:811–818. <https://doi.org/10.1016/j.SNB.2010.08.027>
- Oberti S, Neild A, Wah Ng T (2009) Microfluidic mixing under low frequency vibration. *Lab Chip* 9:1435. <https://doi.org/10.1039/b819739c>
- Pang W, Zhao H, Kim ES et al (2012) Piezoelectric microelectromechanical resonant sensors for chemical and biological detection. *Lab Chip* 12:29–44. <https://doi.org/10.1039/C1LC20492K>
- Qu H, Yang Y, Chang Y et al (2017) On-chip integrated multiple microelectromechanical resonators to enable the local heating, mixing and viscosity sensing for chemical reactions in a droplet. *Sens Actuators B Chem* 248:280–287. <https://doi.org/10.1016/j.snb.2017.03.173>
- Samiei E, Tabrizian M, Hoorfar M (2016) A review of digital microfluidics as portable platforms for lab-on-a-chip applications. *Lab Chip* 16:2376–2396. <https://doi.org/10.1039/C6LC00387G>
- Stokes GG (1845) On the theories of the internal friction of fluids in motion, and of the equilibrium and motion of elastic solids. *Math Phys Pap* 18:75–129. <https://doi.org/10.1017/CBO9780511702242.005>
- Suh YK, Kang S (2010) A review on mixing in microfluidics. *Micromachines* 1:82–111. <https://doi.org/10.3390/mi1030082>
- Tsai JH, Lin L (2002) Active microfluidic mixer and gas bubble filter driven by thermal bubble micropump. *Sens Actuators A* 97–98:665–671. [https://doi.org/10.1016/S0924-4247\(02\)00031-6](https://doi.org/10.1016/S0924-4247(02)00031-6)
- Valencia PM, Basto PA, Zhang L et al (2018) Single-step assembly of homogenous lipid polymeric and lipid quantum dot nanoparticles enabled by microfluidic rapid mixing. <https://doi.org/10.1021/nn901433u>
- Vieffhues M, Eichhorn R, Fredrich E et al (2012) Continuous and reversible mixing or demixing of nanoparticles by dielectrophoresis. *Lab Chip* 12:485–494. <https://doi.org/10.1039/C1LC20610A>
- Wang J, Chen W, Sun J et al (2014) A microfluidic tubing method and its application for controlled synthesis of polymeric nanoparticles. *Lab Chip* 14:1673–1677. <https://doi.org/10.1039/C4LC00080C>
- Wang Z, Zhang H, Yang Y et al (2017) Wireless controlled local heating and mixing multiple droplets using micro-fabricated resonator array for micro-reactor applications. *IEEE Access* 5:25987–25992. <https://doi.org/10.1109/ACCESS.2017.2766270>
- Whitesides GM (2011) What comes next? *Lab Chip* 11:191–193. <https://doi.org/10.1039/C0LC90101F>
- Wiklund M (2012) Acoustofluidics 12: biocompatibility and cell viability in microfluidic acoustic resonators. *Lab Chip* 12:2018. <https://doi.org/10.1039/c2lc40201g>
- Xie Y, Ahmed D, Lapsley MI et al (2012) Single-shot characterization of enzymatic reaction constants  $K_m$  and  $k_{cat}$  by an acoustic-driven,

- bubble-based fast micromixer. *Anal Chem* 84:7495–7501. <https://doi.org/10.1021/ac301590y>
- Yang Z, Matsumoto S, Goto H et al (2001) Ultrasonic micromixer for microfluidic systems. *Sens Actuators A* 93:266–272. [https://doi.org/10.1016/S0924-4247\(01\)00654-9](https://doi.org/10.1016/S0924-4247(01)00654-9)
- Yeo LY, Friend JR (2014) Surface acoustic wave microfluidics. *Annu Rev Fluid Mech* 46:379–406. <https://doi.org/10.1146/annurev-fluid-010313-141418>
- Zhang Z, Wang Y, Zhang H et al (2017) Hypersonic poration: a new versatile cell poration method to enhance cellular uptake using a piezoelectric nano-electromechanical device. *Small* 13:1–10. <https://doi.org/10.1002/sml.201602962>

**Publisher's Note** Springer Nature remains neutral with regard to jurisdictional claims in published maps and institutional affiliations.